A Novel Thin Film Composite Hollow Fiber Osmotic Membrane with One-step Prepared Dual-Layer Substrate for Sludge Thickening

Daniel Yee Fan Ng[1,2], Bing Wu[1,5], Yunfeng Chen[1], Zhili Dong[4], Rong Wang[1,3*]

1. Singapore Membrane Technology Centre, Nanyang Environment and Water Research Institute, Nanyang Technological University, 1 Cleantech Loop, CleanTech One #06-08, Singapore 637141

2. Interdisciplinary Graduate School, Nanyang Technological University, 50 Nanyang Avenue, Singapore 639798

3. School of Civil and Environmental Engineering, Nanyang Technological University, 50 Nanyang Avenue, Singapore 639798

4. School of Material Science and Engineering, Nanyang Technological University, 50 Nanyang Avenue, Singapore 639798

5. Faculty of Civil and Environmental Engineering, University of Iceland, Hjardarhagi 2-6, IS-107 Reykjavik, Iceland

[*]Corresponding author:

Rong Wang, rwang@ntu.edu.sg

Phone: 65-67905327

Graphical abstract

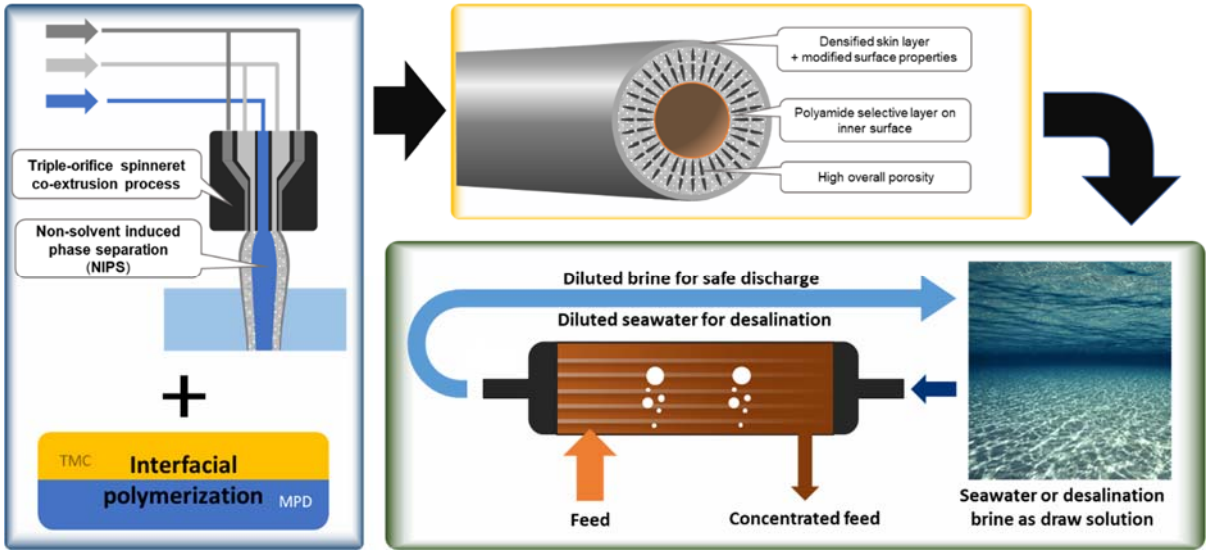

Abstract

Forward osmosis (FO) membranes have received attention as an energy-efficient and low-cost technique in stream concentrating processes. In this work, a novel double-skinned hollow fiber thin film composite (TFC) FO membrane has been successfully fabricated, which consists of a one-step prepared dual layer substrate and a thin inner selective layer formed via interfacial polymerization. The substrate consists of a relatively dense ultrafiltration (UF) outer layer and a porous UF inter layer, both of which were constructed from polyethersulfone (PES) as the substrate material by using dual-layer co-extrusion technique. Compared to the commercial and reported double-skinned FO membranes, the FO membrane developed in this work exhibited a higher permeate flux with humic acid solution as feed. Furthermore, the double-skinned FO membrane was applied in concentrating activated sludge using 0.5 M NaCl as draw solution, and a permeate flux at 5.4 L/m^{2}h was achieved after 5 h operation, which was higher than or comparable to those of the reported FO membranes. Membrane autopsies and foulant analysis suggested that the dense UF skin layer helped to reject greater-sized organic foulants (> 300 Da). This study shed light on the important fabrication features and promising application of the double-skinned hollow fiber TFC FO membrane in sludge concentration.

Key words: Co-extrusion technique; Forward osmosis; Fouling control; Membrane fouling; Sludge thickening

1. Introduction

Forward osmosis (FO) membrane process, which is driven by the difference in osmotic pressure across the membrane, has received much attention in recent years [1-3]. FO process has been proposed as a potential solution, either on its own or integrated with other separation process, in desalination [1, 4-7], wastewater treatment and resource reclamation [7-9], landfill leachate treatment [10], direct fertigation [11] as well as enrichment process of liquid food or other high value-added feed streams [12-14]. Owing to its lower fouling propensity and lower energy consumption, it is particularly suitable for concentrating challenging feed streams which are difficult to be processed with other membrane separation techniques. One of such examples is sludge produced from wastewater treatment process, which has high water content that needs to be removed to facilitate its disposal or other post-treatment processes [15-18].

Large amounts of sewage sludge were generated worldwide, and sludge management may constitute more than 50% of the construction and operating costs of a wastewater treatment plant (WWTP) [15, 17, 19]. Generally, anaerobic digestion (AD) is used to degrade the organic matter in sewage sludge and convert them into biogas [20], followed by volume reduction of digested sludge via coagulation agent and filter press [19]. Alternatively, sludge thickening may be performed prior to digestion process to increase the organic content of sludge and improve the digestion efficiency [21]. Traditional sludge thickening and dewatering technologies cannot retain the soluble matter, and nutrient-rich concentrate would be produced, which requires further treatment to meet the discharge requirement [17]. As such, FO process may be

77 considered as a potential solution which could achieve sludge volume reduction and
78 nutrient retention simultaneously.

79 In the earlier studies on sludge thickening and dewatering using FO process, it has
80 been proposed to use seawater reverse osmosis (SWRO) brine or seawater as draw
81 solutions [15, 17, 18]. In addition to providing a higher driving force in FO process, the
82 SWRO brine will be diluted before discharged back into sea, which could avoid
83 negative environmental impact of direct brine discharge [22]. Meanwhile, the
84 regeneration of the draw solution becomes unnecessary, thus greatly reduce the
85 overall energy consumption of FO process. Alternatively, the diluted seawater can be
86 reused as feed again in seawater desalination process to produce potable water [23,
87 24], which allows simultaneously concentrating waste sludge and desalinating
88 seawater at high recovery.

89 In previous studies, the flat sheet FO membranes operated at active layer facing feed
90 solution (AL-FS) have been documented for sludge concentration [15-18, 21]. It is well
91 known that compared with flat sheet FO membranes, hollow fiber FO membranes offer
92 several advantages, such as mechanically self-supported nature, favourable flow
93 pattern during filtration and high packing density [25]. It is also noted that most of
94 commercial TFC hollow fiber membranes possess a polyamide selective layer on the
95 lumen side as it is technically feasible to achieve homogenous distribution of monomer
96 solutions in the lumen side during interfacial polymerization. Unexpectedly, in the AL-
97 FS orientation, the greater-sized particulates in the sludge could easily clog the lumen
98 of hollow fiber (inner diameter of around 1 mm or less). Thus, AL-DS orientation is
99 adopted for hollow fibre FO operation in sludge concentration. However, severe

membrane fouling is inevitable as the smaller-sized substances in the sludge could potentially penetrate and accumulate in the porous substrate.

In order to prevent the penetration of foulants into the porous support layer, one solution is to narrow down the pore size on the support side of FO membrane by adjusting the fabrication conditions (such as increasing the polymer concentration in dope solution). However, it would inevitably reduce the overall porosity of the porous support layer. As a result, internal concentration polarization (ICP) may become more severe and membrane permeability would be relatively low. Alternatively, addition of another relatively dense layer on the porous substrate to form a double-skinned FO membrane has been proposed [26-30]. The primary selective layer would possess sufficient selectivity to draw solutes, while the other selective layer serves as the barrier against the penetration of foulants. Meanwhile, the properties of the porous support layer sandwiched between two selective layers are remained. The additional dense layer of TFC hollow fiber membranes was generally introduced on shell side by interfacial polymerization [29], chemical cross-linking [27] or layer-by-layer (LBL) assembly [28, 31] before or after the formation of a selective layer at lumen side. The previously-reported methods required three or more fabrication steps, which inevitably increase the complexity of fabrication process and the cost of membrane production.

In this study, a novel double-skinned hollow fiber TFC FO membrane was fabricated by a two-step preparation. The substrate possessed a relatively dense ultrafiltration(UF)-like outer skin layer and a relatively porous UF inner layer, which were formed simultaneously via one-step co-extrusion technique based on non-solvent induced phase separation (NIPS) [32]. The inner-selective layer was formed on the porous lumen-side support layer by interfacial polymerization. Furthermore, the

newly developed double-skinned hollow fiber FO membrane was characterized by a series of standard protocols and its performance was benchmarked against the commercial membrane and double-skinned hollow fiber membranes reported in literature. The fouling mechanisms for the hollow fiber FO membrane in concentrating sludge were also illustrated. This study aims to explore an effective FO membrane fabrication technique and demonstrate the promising application of the double-skinned hollow fiber FO membrane in sludge concentration.

2. Materials and methods

2.1. Materials

Polyethersulfone (PES, Gafone^{TM} 3000P, Solvay, Belgium), N-methyl-2-pyrrolidone (NMP, Merck Chemicals, USA), polyethylene glycol 200 (PEG, Mw = 200 g/mol, Merck Chemicals, USA), acetone (Merck Chemicals, USA), polyvinylpyrrolidone (PVP, Mw = 1,300,000 g/mol, Acros Organics, USA), glycerol (85%, Merck Chemicals, USA) and DI water was used for the fabrication of hollow fiber substrates. ε-caprolactam (Merck Chemicals, USA), cyclohexane, 1,3,5-benzenetricarbonyl trichloride (TMC, Sigma-Aldrich, USA), m-phenylenediamine (MPD, Sigma-Aldrich, USA), sodium dodecyl sulfate (SDS, Sigma-Aldrich, USA) and DI water were used in the fabrication of TFC membrane via interfacial polymerization. Polyethylene glycol (PEG) of various molecular weights ranging from 200 to 20,000 g/mol (Merck Chemicals, USA) was used to characterize the molecular weight cut-off (MWCO), mean pore size and pore size distribution of the hollow fiber substrates. Sodium chloride (NaCl, Merck Chemicals, USA), humic acid sodium salt (HA, Sigma-Aldrich, USA) were used for the preparation of draw and feed solutions used in the characterization of TFC membrane

intrinsic properties and FO tests. Deionized (DI) water was obtained by a Milli-Q system (Millipore, USA) and used to prepare all aqueous solutions in this study.

2.2. Fabrication of PES hollow fiber substrates

PES was dried in vacuum oven at 50°C overnight before it was used for the preparation of dope solution. To prepare the dope solution, PES was dissolved into NMP with constant stirring at 60 °C for 1 h. After the polymer was completely dissolved, the additives were added into the dope solution and the mixture was stirred until a homogeneous solution was obtained. Subsequently, the dope solutions were slowly cooled down to room temperature and degassed under vacuum overnight prior to hollow fiber spinning process. The dope compositions used in fabricating PES hollow fiber substrate are listed in Table 1. To evaluate the stability of the polymer dopes, water was added slowly into polymer dopes (which were prepared separately) under constant stirring until clouding of polymer dope was observed. The mass concentration of water required to trigger clouding phenomenon was recorded as the cloud point of the polymer dope.

Table 1. Dope compositions in fabricating PES hollow fiber substrate

Polymer dope	Composition (wt%)						Cloud point (wt% of H_2O)
	PES	NMP	PEG	Acetone	PVP	DI water	
PES#1 (Inner dope)	20.0	40.0	40.0	-	-	-	4.2
PES#2 (Outer layer)	29.2	50.3	-	16.8	1.0	2.8	4.2

PES hollow fiber substrates were fabricated through dry-jet wet-spinning process through the NIPS. The details of the procedures can be found in literature [25]. The substrate was prepared from simultaneous co-extrusion of two different polymer dopes, where the skin structure on the shell side was densified through increased polymer

concentration and exclusion of pore-forming additives to reduce the surface pore size of the substrate. The detailed spinning conditions are listed in Table 2.

Table 2. Spinning conditions for fabricating PES hollow fiber substrates

Spinneret dimension	
Bore channel inner diameter (μm)	360
Middle channel inner/outer diameter (μm)	620/890
Outer channel inner/outer diameter (μm)	1230/1420
Spinning conditions	
Bore fluid composition	DI water
Bore fluid low rate (mL/min)	10
Inner dope composition	PES#1
Inner dope flow rate (mL/min)	6.7
Outer dope composition	PES#2
Outer dope low rate (mL/min)	0.10
Take up speed (m/s)	0.27
Air gap (cm)	1.0
Room temperature (˚C)	23-24
Coagulation bath temperature (˚C)	22-23
Relative humidity (%)	70

2.3. Characterization of PES hollow fiber substrate

The standard protocol of hollow fiber substrate characterization was described previously [25, 33]. Specifically, the dimension of the hollow fiber membrane was determined with a digital optical microscope (Keyence, Japan). The structure and morphology of the hollow fiber membranes were measured by using a field emission scanning electron microscope (FE-SEM, Jeol, Japan) after the membranes were freeze-dried and coated with platinum. The average overall porosity of the hollow fiber substrate was determined using the gravimetric method by measuring the mass of water that was contained in membrane pores.

The pure water permeability (PWP) of the hollow fiber substrate was examined by employing DI water circulating through the shell and lumen sides of the membrane module at 1 bar. The MWCO of the hollow fiber substrate was determined by using

solute rejection experiments, in which 200 mg/L PEG solutions (with different molecular weights) was circulated over the hollow fiber substrate under 1 bar of transmembrane pressure (TMP) in the cross-flow filtration testing system. The feed and permeate samples were collected and analysed by using gel permeation chromatography (GPC) instrument equipped with refractive index (RI) detector (Polymer Laboratories-GPC 50 plus system, Agilent, USA). The MWCO, pore size and pore size distribution of hollow fiber substrate were then calculated from the solute rejection based on the procedures reported elsewhere [34, 35].

2.4. Interfacial polymerization on PES hollow fiber substrate

The PES hollow fiber substrate was immersed in a 50 wt% glycerol solution for 1 day and dried in air for 1 day prior to being used for preparation of TFC membranes via interfacial polymerization. Then, hollow fiber substrate modules were made by placing 5 pieces of hollow fibers in each module casing assembled from two PP T-fittings connected by PTFE tubes (1/2 inch outer diameter, 3/8 inch inner diameter), where the gaps at two ends were sealed with epoxy adhesive (ARALDITE Rapid 5 minutes). The effective length of the hollow fibers in each module was around 25 cm, and the effective membrane area was around 38 cm^2. The selective layer was formed on the lumen side of the hollow fiber through interfacial polymerization, as described elsewhere [25, 36]. In detail, the lumen of PES hollow fiber substrate was filled with MPD solution to allow the penetration of the monomer and additives into the substrate. After removing the residual MPD solution from the fiber lumen, the TMC in cyclohexane was pumped through the fiber lumen of the membrane. The TFC membrane, denoted as “PES-HF-TFC”, was immersed in DI water for one day before use.

208 *2.5. TFC hollow fiber intrinsic properties and FO membrane performance evaluation*

209 Water permeability coefficient (A, L/m^{2}h/bar, LMH/bar) of the PES-HF-TFC membrane
210 was determined and calculated in the same way as the PWP of the hollow fiber
211 substrate. Salt rejection (R_s, %) of the PES-HF-TFC membrane was determined by
212 circulating 500 ppm NaCl solution through the membrane lumen under 1 bar, where
213 the conductivity of feed (EC_{feed}) and permeate (EC_{perm}) were measured using
214 conductivity meters (Mettler Toledo, Switzerland). The detailed procedures for
215 determination of salt rejection and salt permeability coefficient (B, L/m^{2}h,LMH) can be
216 found elsewhere [37].

217 A bench-scale FO testing system was employed to examine the FO performance of
218 the PES-HF-TFC membrane in the AL-DS orientation by using a 0.5 M NaCl solution
219 as draw solution, while DI water was used as feed. The details of the setup were
220 described previously [38]. For the evaluation of FO performance, the osmotic-driven
221 water flux (J_w, L/m^{2}h, LMH) was determined based on the following equation [33]:

222 $$J_w = \frac{\Delta w}{A_m \rho_w \Delta t} \quad (1)$$

223 where Δw (kg) is the change in feed weight over Δt (h); A_m (m^2) is the effective
224 membrane area; ρ_w (kg/L) is the density of water. The salt reverse flux (J_s, g/m^{2}h, gMH)
225 was examined according to the following equation:

226 $$J_s = \frac{C_t V_t - C_0 V_0}{A_m \Delta t} \quad (2)$$

227 where C_0 (g/L) and V_0 (L) are the salt concentration and feed volume at time 0; C_t and
228 V_t indicate the final salt concentration and feed volume over Δt, respectively. The

specific reverse salt flux is calculated based on the ratio of salt flux to water flux (J_s/J_w, g/L). Duplicate experiments (n=2) were performed and averaged data were presented in the table.

To assess the fouling propensity of the PES-HF-TFC membrane, the model foulant humic acid (Sigma-Aldrich, 50 mg/L) was employed as feed solution and 0.5 M NaCl was used as draw solution. As shown in Figure 1, the feed solution was circulated over the shell side of the PES-HF-TFC membrane at a flow rate of 1 L/min (corresponding to crossflow velocity of 0.23 m/s) and the draw solution was circulated through the lumen side of the membrane at a flow rate of 190 mL/min (corresponding to crossflow velocity of 0.8 m/s), i.e., in the AL-DS orientation. After each 5-h FO experiment with humic acid-containing feed, physical cleaning was applied by flushing the shell side of the fiber for 30 sec with DI water, and then the recovered performance of the cleaned membrane was evaluated by using DI water as feed. For comparison, the FO performance of the commercially available FO membrane (OsmoF2O™ FO flat sheet membrane, Fluid Technology Solutions, Albany, OR; with effective membrane area of 40 cm^2) was also evaluated in the AL-DS orientation using the same operation condition and cleaning protocol.

2.6. Compositions of feed sludge sample

Anaerobic digested sludge samples were collected from Ulu Pandan Water Reclamation Plant in Singapore and stored at 4°C. The sludge was warmed to room temperature (22-23°C) before use. The composition of feed digested sludge is provided in Table 3.

252 **Table 3.** Compositions of digested sludge used as feed in sludge thickening process

MLSS (g/L)	pH	Conductivity (mS/cm)	DOC (mg/L)	TN (mg/L)	NH_4^+-N (mg/L)	PO_4^{3-}P (mg/L)	Ca (mg/L)	Mg (mg/L)	Si (mg/L)	Osmolality (mOsm/kg)
15.5	7.23	5.15	9.3	543.3	670	558	86.6	40.8	28.9	108

253

254 *2.7. Sludge thickening process by FO membrane*

255 A series of short-term FO sludge thickening experiments were carried out in the AL-
256 DS orientation using 0.5 M NaCl as draw solution (Figure 1). The feed sludge was
257 delivered to the shell side of the PES-HF-TFC membrane and the draw solution was
258 delivered to the lumen side of the membrane at a flow rate of 1 L/min (corresponding
259 to crossflow velocity of 0.23 m/s) and 190 mL/min (corresponding to crossflow velocity
260 of 0.8 m/s), respectively. Physical cleaning was applied after 50 minutes of FO sludge
261 thickening process operation, where the shell side of membrane is flushed with water
262 at crossflow rate of 1.5 L/min for 5 minutes. At the same time, membrane backwashing
263 was also carried out by circulating DI water on the lumen side of the membrane at 1
264 bar pressure. A total of six FO sludge thickening-cleaning cycles were performed.

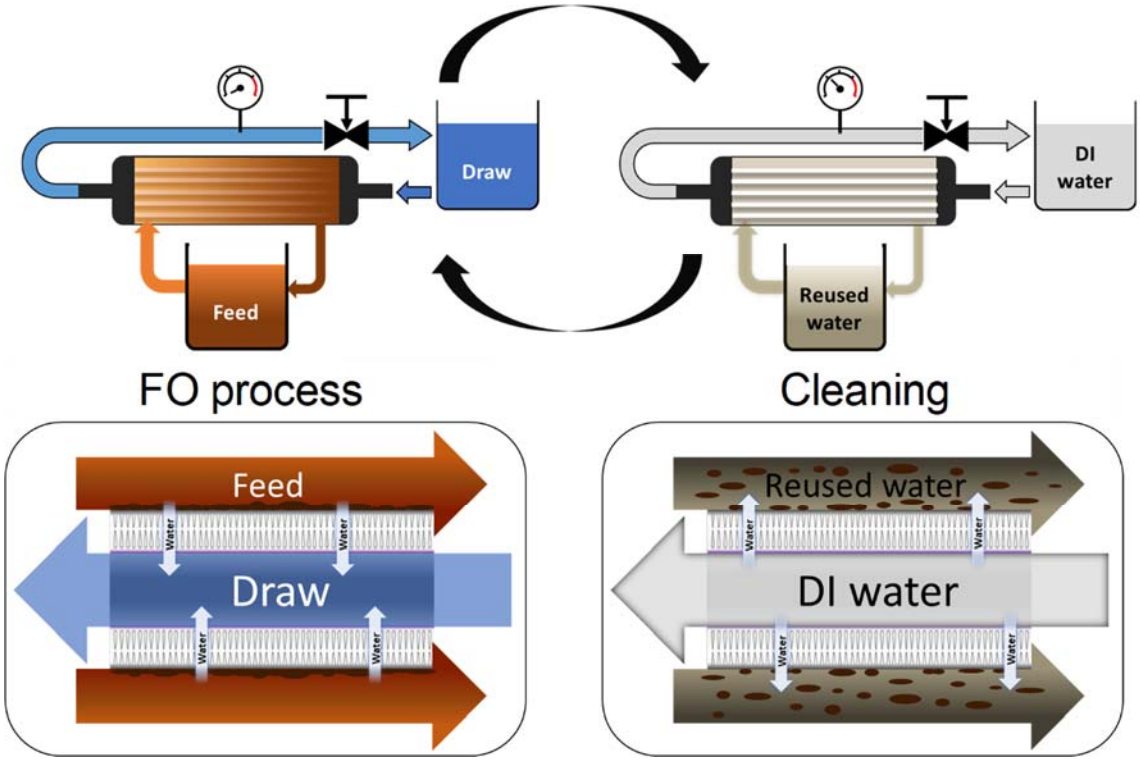

Figure 1. Schematic illustration of the experimental design of FO system operation.

2.8. Extraction of irreversible foulants from membranes

At the end of experiments, the fouled membranes were physically rinsed with DI water to remove loosely-attached foulants (i.e., cake layer foulants) on membrane surface. After that, the fouled membranes were soaked into NaOH solution (pH 12) under constant agitation (by using vortex mixer) for 2 h to extract the organic foulants accumulated inside the porous substrate layer (i.e., chemically removable foulants).

2.9. Characterization of feed samples and foulants

Mixed liquor suspended solids (MLSS) was determined according to Standard Methods [39]. Conductivity and pH were examined by a conductivity/pH meter (Hanna, USA). The feed sample was filtered with a 0.45 μm filter (Pall Corporation, USA), and the dissolved total organic carbon (TOC) and total nitrogen were measured by a

279 TOC/TN analyzer (Shimadzu, Japan). The concentration of NH_4^+ was determined by
280 using commercial test kits and measuring colour intensity with a spectrophotometer
281 (Hach, USA). Organic matter composition analysis was carried out by using liquid
282 chromatography-organic carbon detection (LC-OCD, DOC-Labor, Germany) [40].

283 ## 3. Results and discussion

284 ### *3.1. Characteristics of PES hollow fiber substrate*

285 In this study, PES hollow fiber substrate with porous inner layer and dense outer skin
286 was fabricated by one-step co-extrusion technique with a variation of dope
287 composition (Table 1) and spinning parameter (Table 2). As shown in Figure 2, the
288 hollow fiber substrate exhibited finger-like cross-section morphology, where the
289 macrovoids extended from both lumen and shell sides and intercepted at the centre
290 of the membranes. The thin layers of defect-free skin lying on the surface of both
291 lumen and shell sides are formed, as the result of rapid vitrification (solid-liquid phase
292 separation) during the initial contact between the polymer dope and strong non-solvent.
293 Clearly, as shown in Figure 2d, the two layers formed from different dope compositions
294 fused perfectly with no clear sign of delamination, similarly to those dual-layer
295 membranes based on the simultaneous co-extrusion technique [41, 42]. Generally,
296 similar shrinkage ratios of outer and inner layers in the NIPS process promote the
297 formation of delamination-free structure. In this study, the difference in shrinkage ratio
298 was minimized by employing the same polymer in both outer and inner dopes. Also,
299 the cloud point of the outer dope was adjusted to the same level as the inner dope by
300 the addition of water into the dope, which is believed to have promoted the formation
301 of continuous phase at the interface.

In addition, the skin layer on shell side (i.e., tight UF skin layer) seems to be much thinner than that on the lumen side (i.e., loose UF skin layer). This could be associated with the fact that the higher polymer content in the outer layer dope solution impeded the inward diffusion of water and delayed the vitrification process. Under this scenario, the formation of porous structure close to the skin layer was promoted, that is attributed to the nucleation and growth mechanism [43, 44].

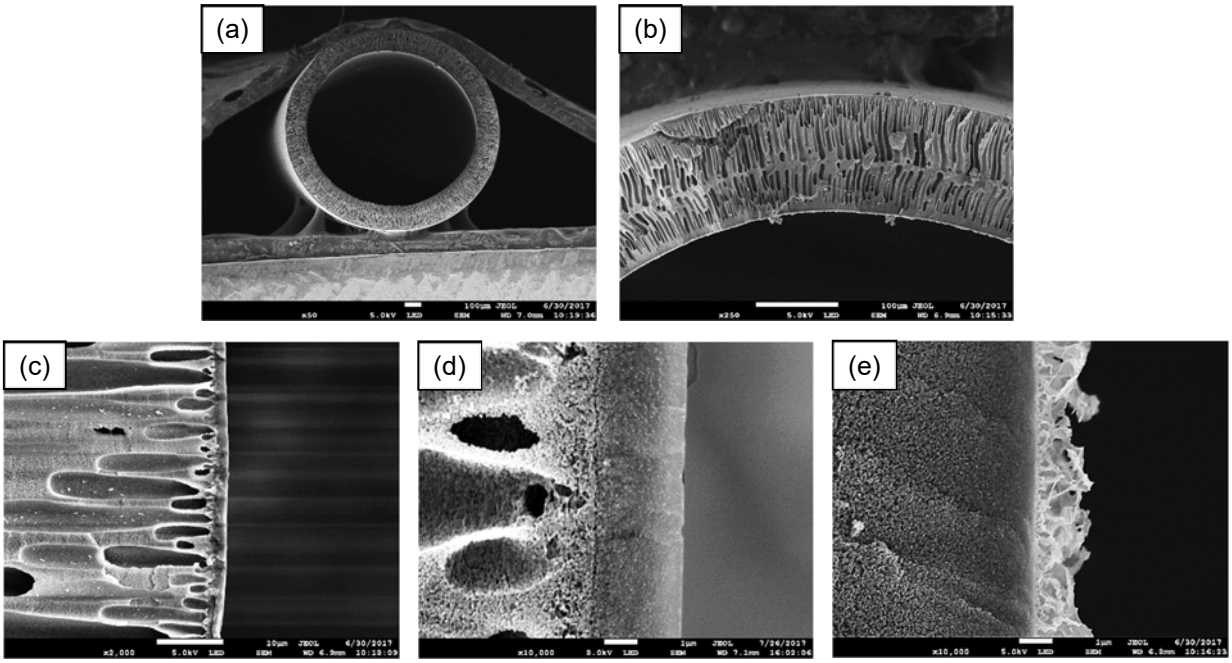

Figure 2. SEM images displaying morphologies of the pristine PES-HF-TFC membrane. (a-b) Overall cross-section; (c) Cross-section on shell side; (d) Magnified cross-section on shell side (dense UF); (e) Magnified cross-section on lumen side showing polyamide selective layer.

The properties of the PES hollow fiber substrate are summarized in Table 4. It had an average inner and outer diameter of 999 μm and 1287 μm, respectively (i.e., a thickness of 144±3 μm). While the substrate had a considerably high porosity of around 75%, its PWP was only 4.6 LMH/bar, which indicated that the outer skin layer has much higher contribution to overall mass transfer resistance. Under an outside-in

filtration mode, the MWCO of the hollow fiber substrate was estimated to be around 1.2 kDa, suggesting that the outer surface of the membrane was completely and evenly covered by the dense skin layer. It is noted that the MWCO of the substrate under inside-out filtration mode was about 32 kDa, which is much higher than that under the outside-in filtration mode. It is well known that the dextran molecules in the feed solution could easily penetrate into the porous matrix of the membrane and accumulate underneath the outer dense skin, which resulted in a concentrative internal concentration polarization and thus a relatively lower apparent rejection.

Table 4. Properties of the pristine PES hollow fiber substrate

Dimension (μm)			PWP (L/m^{2}h bar)	MWCO (kDa)		Mean pore diameter (nm)	Geometric standard deviation	Porosity (%)
Inner diameter	Outer diameter	thickness		[I-O] [a]	[O-I] [b]			
999±6	1287±9	144±3	4.6±1.5	32	1.2	1.25	1.35	74.6±0.3

[a] [I-O] indicates that the membrane properties was tested in inside-out configuration, where the pressurized feed solution was circulated in the lumen side of the membrane.
[b] [O-I] indicates that the membrane properties was tested in outside-in configuration, where the pressurized feed solution was circulated in the shell side of the membrane.

The mean pore diameter was calculated from the solute rejection characterized under outside-in filtration mode, and the probability distribution function curve is shown in Figure 3. Based on the MWCO and pore size distribution, the selectivity of outer skin layer of the hollow fiber substrate can be considered to be within tight UF range (with MWCO between 1 kDa to 3 kDa) [45]. The improved selectivity of the substrate may help to supress membrane fouling caused by pore plugging, which is mostly irreversible through physical cleaning [46, 47]. Such characteristics could help to improve the fouling resistance of inner-selective TFC membrane prepared from this substrate when operating in AL-DS orientation, since the smaller pore size of the outer

skin of the substrate layer would deter the entry and deposition of high molecular weight organic foulants from feed solution into the matrix of the membrane.

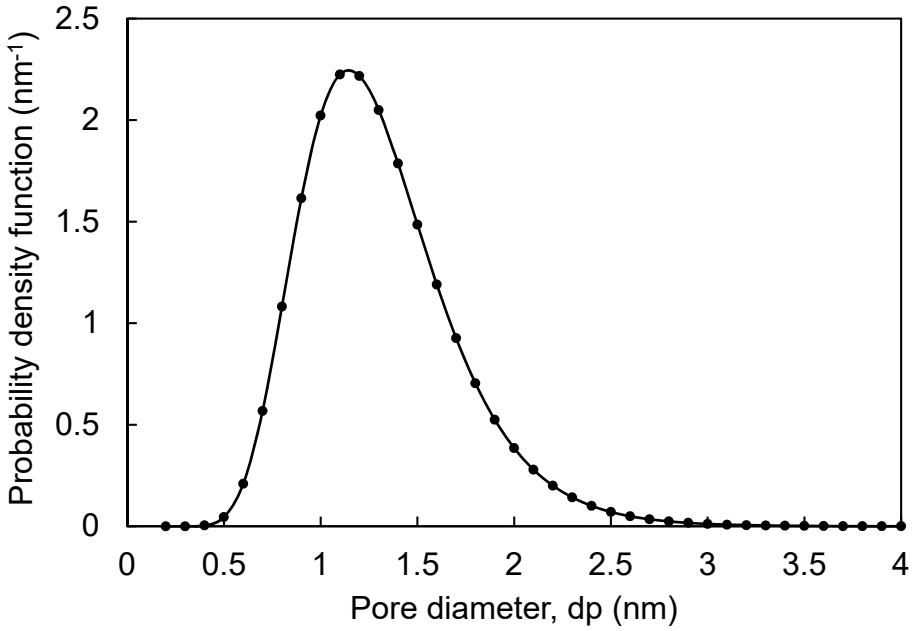

Figure 3. Pore size distribution of the outer skin layer of pristine dual-layer PES hollow fiber substrate.

3.2.1. Membrane morphology

The cross-section view of the polyamide selective layer on the inner surface of the PES-HF-TFC membranes is shown in Figure 2e. Similar to the TFC hollow fiber membranes reported in some other studies [28, 33, 48], the selective layer was laid on the porous support layer as an extra layer and displayed typical ridge and valley pattern.

3.2.2. Membrane performance: DI water as feed solution

The performance of the PES-HF-TFC membrane with DI water as feed solution in the AL-DS orientation was characterized. When 0.5 M NaCl was used as the draw solution, the water flux and reverse salt flux of PES-HF-TFC membrane was 24.1 LMH and 8.4

gMH, respectively (Table 5). Compared to other reported double-skinned FO membranes, the clean water performance of this membrane in terms of water and reverse salt fluxes was not superior (Table 5). It should be noted that such FO performance may not be indicative in a situation with real feed solutions. Therefore, the performance of the membrane was further assessed in the following sections with humic acid and activated sludge as feed solutions.

3.2.3. Membrane performance: humic acid as feed solution

The FO membrane performance in the AL-DS orientation was examined by using humic acid as feed solution, a model foulant which has been employed in several earlier studies [49-51]. The water flux profile of the PES-HF-TFC membrane in three FO filtration-physical cleaning cycles is presented in Figure 4. In the first cycle, the water flux decreased linearly over time, approaching 75% of pristine membrane water flux after 5 h. In the following two cycles, the water flux decline rate appeared to be slower than the first cycle. The drop of water flux might be caused by (1) deposition of the high molecular weight fraction of humic acid forming a thin cake layer and the partial pore blocking by low molecular weight fraction of humic acid [50]; and (2) an decrease in osmotic pressure due to the accumulation of draw solutes in feed solution.

It is noted that the short-term physical cleaning (30 sec) of the PES-HF-TFC membrane could contribute to above 82% recovery of water flux during cycles 2 and 3, implying that cake layer fouling was predominant for the PES-HF-TFC membrane during long term operation. Nevertheless, after 15-h filtration, compared to the commercial OsmoF2O™ membrane with humic acid as feed solution in the AL-DS orientation (water flux at ~5.6 LMH), the PES-HF-TFC membrane (water flux at >14.1

LMH) displayed much better membrane performance when the same concentration of draw solution (0.5 M NaCl) was employed (Figure 4).

To make a fair comparison, the same initial water fluxes of PES-HF-TFC and commercial OsmoF2O™ membranes were set by regulating the draw solution concentration (0.5 M NaCl for PES-HF-TFC membrane and 2 M NaCl for commercial OsmoF2O™ membrane) and the water fluxes of the two membranes using humic acid as feed were recorded in Figure 4. After 3 cycles, OsmoF2O™ membrane had slightly higher water flux than the PES-HF-TFC membrane. However, short-term physical cleaning could only recover less than 7% of water flux for the OsmoF2O™ membrane, implying predominant irreversible fouling. It is reported that humic acid could cause pore clogging in a porous support layer in the AL-DS orientation due to comparable sizes of humic acid and support layer pore size, which resulted in enhanced ICP and increased membrane resistance [50]. Also, the rather pronounced water flux decline in PES-HF-TFC membrane tested with humic acid may be attributed to adsorptive fouling [52]. Due to the lower hydrophilicity of PES, adsorption of humic acid onto the surface of PES outer skin layer occurs more readily and leads faster increase in membrane resistance.

These findings indicated that the dense outer skin of PES-HF-TFC membrane fabricated in the current study, which was purposefully modified to reduce the average surface pore size (with mean pore diameter of 1.25 nm), could effectively restrict the penetration of high molecular weight humic acids (its hydration radius was estimated to be between 2.3 nm and 7.7 nm solution [53]) into the support layer and mitigated irreversible fouling. It also reveals a possibility to achieve sustainable long-term operation of PES-HF-TFC membrane by employing periodic physical cleaning.

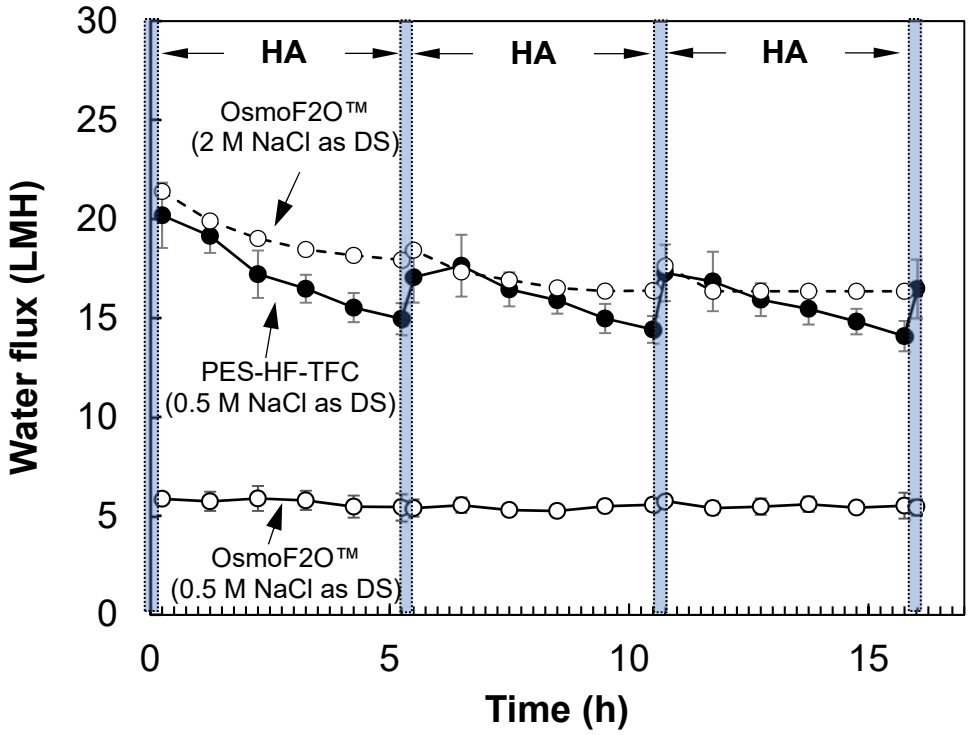

404

405 **Figure 4.** FO performance of PES-HF-TFC and OsmoF2O™ FO membrane with
406 humic acid (50 mg/L) as feed. The crossflow velocity on lumen side and shell side was
407 at 0.8 m/s and 0.23 m/s, respectively). Shaded region indicate that physical cleaning
408 was carried out and then the FO water flux of cleaned membrane was tested by using
409 DI water as feed.

410

411 *3.2.4. Comparison with double-skinned FO membranes in literature*

412 The FO performances of the double-skinned FO membrane developed in this study
413 and those reported in the literatures using humic acid as the model foulant are
414 summarized in Table 5. Apparently, although the osmotic pressures in these previous
415 studies were much higher than that in this study, the permeate flux of the PES-HF-
416 TFC membrane was higher than or comparable to most of previous studies using the
417 double-skinned FO membranes [49] or commercial FO membranes [54-56]. However,
418 Fang et al. [28] from our group reported a double-skinned hollow fiber membrane (RO-
419 like polyamide TFC selective layer on inner surface and NF-like crosslinked

polyelectrolyte LBL selective layer on outer surface) with a higher permeate flux (~23.6 LMH) at the same osmotic pressure (0.5 M NaCl) as in this study. This is likely due to (1) much thinner LBL selective layer than the dense UF skin layer in current study; (2) the stronger humic acid-PES membrane interaction because of lower hydrophilicity of PES compared to the LBL layer, which led to faster deposition of humic acid on the outer surface of the membrane; (3) the improved humic acid rejection effectiveness of the NF-like layer compared to the dense UF-like layer, which possibly resulted in less internal concentration polarization and irreversible fouling. Nevertheless, it should be pointed out that the current method of making double-skinned hollow fiber membrane is less complex in procedure. The PES-HF-TFC membrane developed in this study exhibited moderate fouling reversibility, as depicted by the reproducible water flux profile over consecutive cycles of FO experiments (Figure 4). To further reduce irreversible fouling when the dual-layer FO membrane is operated in the AL-DS orientation, improving surface hydrophilicity and minimizing surface pore size of the secondary rejection layer by optimization of membrane fabrication process is suggested. One simplistic approach to achieve such goal is to blend hydrophilic additives (such as PES block-copolymers with hydrophilic segments) during dope preparation process, such that inherently more hydrophilic substrates may be fabricated. In addition, such approach could be adopted to modify only the outer dope composition when fabricating hollow fiber substrates with dual-layer co-extrusion technique.

~~In addition, several fouling control approaches can be applied to control irreversible fouling on currently developed double-skinned FO membranes, such as feed pre-treatment, periodic chemical cleaning, coating an additional adsorption layer (such as powdered activated carbon) on membrane surface.~~

Table 5. Performance comparison of various TFC FO membranes using humic acid as feed solution

Membranes	Selective layer properties	Intrinsic properties			FO performance				Ref.
		A (LMH/bar)	R_s (%)	B (LMH)	Orientation	Draw	Feed	Water flux (LMH)	
Inner-selective PES-TFC hollow fiber membrane with densified outer skin	Tight-UF outer skin (PES), RO-like polyamide TFC (MPD-TMC) selective layer on inner surface	2.29	89	0.16	AL-DS	0.5 M NaCl	Humic acid (50 mg/L)	~14.1 after 5 h	Current work
Double-skinned flat sheet membrane	TFN (DA-TMC-CNT) selective layer on both top and bottom surface	-	-	-	AL-DS	2.0 M $MgCl_2$	Humic acid (5 mg/L)	~9.9 [g] after 3 h	[49]
Double-skinned hollow fiber membranes	RO-like polyamide TFC (MPD-TMC) selective layer on inner surface, NF-like crosslinked LBL (PSS-PAH) selective layer on outer surface	2.01 [a]	95.4 [b]	0.16 [b]	AL-DS	0.5 M NaCl	Humic acid (200 mg/L) and 10 mM NaCl	~ 23.6 [h] after 4 h	[28]
Inner selective SPES-TFC FO membrane (Samsung Cheil Industries, Korea)	TFC selective layer on inner surface	-	-	-	AL-FS	2.0 M KCl	Humic acid (60 mg/L)	~13.9 [i] after 5 h	[55]
Asymmetric CTA flat sheet membrane (HTI, Albany, OR)	CTA selective layer (RO) with embedded polyester mesh	0.517 [c]	-	0.195 [d]	AL-FS	2.0 M NaCl	Humic acid (60 mg/L as DOC)	~13.1 [j] after 5 h	[54]
					AL-DS		Humic acid (60 mg/L as DOC)	~19.6 [j] after 5 h	
TFC FO membrane (Oasys Water, Boston, MA)	RO-like polyamide selective layer	4.70 [e]	-	0.164 [f]	AL-DS	1.0 M NaCl	Humic acid (100 mg/L in background electrolyte solution)	~15.5 [k] after 5 h	[56]

[a] Test conditions: RO test at 2.0 bar applied pressure; DI water as feed.
[b] Test conditions: RO test at 2.0 bar applied pressure; 500 ppm NaCl as feed.
[c] Test conditions: RO test at 0 -15.5 bar applied pressure; DI water as feed.
[d] Test conditions: RO test at 0-15.5 bar applied pressure; 10 mM NaCl as feed.
[e] Test conditions: RO test at 8.62 bar applied pressure; feed temperature 20 °C; DI water as feed.
[f] Test conditions: RO test at 8.62 bar applied pressure; feed temperature 20 °C; 2000 mg/L NaCl as feed.
[g] Test conditions: crossflow velocity was 1.59 cm/s for both draw and feed.
[h] Test conditions: cross-flow velocity was 10 cm/s for both feed and draw, room temperature (23 °C), all solutions exhibited neutral pH of ~7.
[i] Test conditions: crossflow Reynolds number for feed and draw were 1900 and 700, respectively and temperature was 25 ± 0.5 °C.
[j] Test conditions: crossflow rate were 0.19 L min^{-1} (corresponding to a crossflow velocity of 9.8 cm/s) for both feed and draw; with membrane supported by mesh; temperature at 20 °C; pH = 6.5; ionic strength = 1 mM.
[k] Test conditions: cross-flow rates of feed and draw were 1 L/min (corresponding to cross-flow velocity of 9 cm/s); temperatures of feed and draw solutions were 25 ± 1 °C.

3.3. FO performance in a sludge concentrating process

3.3.1. Membrane performance

Generally, activated sludge contains greater-sized solids (having sizes up to a few millimetres) and can easily clog the hollow fiber membrane lumen side (i.e., active layer) in the AL-FS direction. Therefore, in this study, the sludge concentrating tests were performed in the AL-DS orientation and the dense nature of UF skin on the feed

solution side is expected to play a critical role in reducing the membrane fouling propensity.

The membrane performance in six filtration-physical cleaning cycles is recorded in Figure 5. The water flux of the PES-HF-TFC membrane dropped significantly during the first cycle. After that, slowly declining water flux was observed. At the end of each cycle, physical cleaning (flushing with backwashing for 5 min) was applied, which resulted in merely 2.6-4.8% of water flux recovery. This hints that the cake fouling has a negligible contribution to water flux decline, while irreversible fouling was predominant. To further explore the membrane fouling mechanism, after 5-min physical cleaning, the SEM images of the fouled membrane were taken (Figure 6). It is observed that very limited foulants were deposited on the fouled membrane surface, which suggests that pore blocking or narrowing predominantly caused flux decline rather than physical-irremovable cake layers (such as gel layers). This observation was inconsistent with the finding in concentrating sludge in the AL-FS direction, in which reversible cake layer fouling was a major contributor to membrane flux decline [17, 18]. It appears that the operation orientation plays an important role in affecting membrane fouling mechanisms.

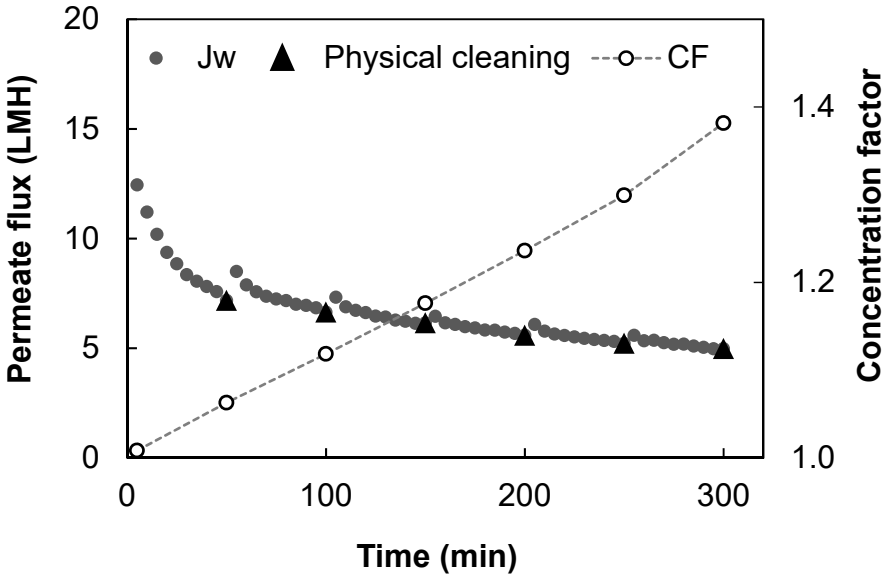

Figure 5. The PES-HF-TFC membrane performance with activated sludge as feed (0.5 L of feed sludge, 0.5 M NaCl was used as the draw solution. The crossflow velocity on lumen side and shell side was at 0.8 m/s and 0.23 m/s, respectively).

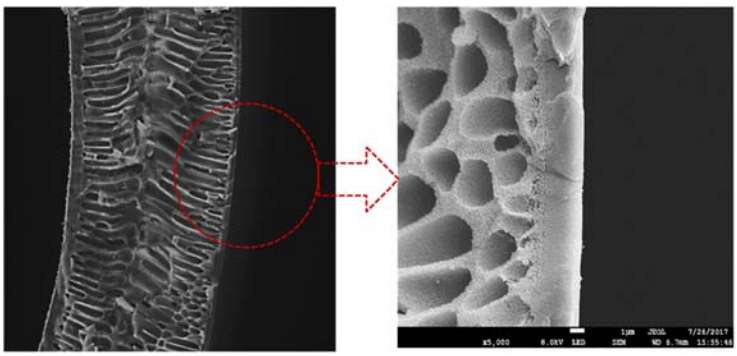

Figure 6. The SEM images of the feed side (tight UF) of the fouled membrane after the sludge concentrating test (300-min) and 5-min physical cleaning.

After 300-min of operation, the sludge was concentrated at 1.4 times and the water flux of PES-HF-TFC membrane was stabilized at ~5.2 LMH with ~24.6 bar of osmotic pressure driving force. The achieved water flux per osmotic pressure (~0.21 LMH/bar) in this study at the AL-DS orientation was higher than those using commercial TFC and CTA FO membranes reported in the literatures at the AL-FS orientation (~0.06-0.19 LMH/bar; Table 6). It is worth noting that the initial sludge concentration (15.5 g/L)

employed in this study was 1 to 7 times higher of those in the reported literatures. It can be expected to achieve even higher permeate flux (> 5.2 L/m^2h) for the PES-HF-TFC membrane when a lower concentration of sludge is used. The combination of high water flux and low fouling tendency offers the possibility for such membranes to be used in concentrating sludge or other high solids contained feed solutions and in recovering valuable products.

Table 6. A summary of operation conditions and membrane performances of various FO-based sludge thickening processes

Membrane	Orientation	Draw solution	Draw osmotic pressure [a] (bar)	Initial MLSS (g/L)	Final MLSS (g/L) @ 5h	Water flux (LMH) @ 5h	Ref.
TFC, hollow fiber	AL-DS	0.5 M NaCl	~24.6	15.5	21.8	5.2	This work
CTA, flat sheet (HTI, Albany, Oregon, US)	-	1.5 M $MgCl_2$	~111	1.8	~2.5 [b]	-	[57]
CTA, flat sheet (HTI, Albany, Oregon, US)	AL-FS	Simulated SWRO retentate (mixed inorganic salts)	~40	7.3	~24 [c]	-	[18]
CTA, flat sheet (HTI, Albany, Oregon, US)	AL-FS	Simulated seawater (0.62 M NaCl)	~30.3	8.0	~14.9 [c]	~5.1 [d]	[17]
CTA, flat sheet (HTIs OsMem™, Albany, Oregon, US)	AL-FS	Simulated seawater (0.62 M NaCl)	~30.3	8.0	~13.4 [c]	~5.6 [d]	[15]
CTA, flat sheet (HTI, Albany, Oregon, US)	AL-FS	0.7 M EDTA sodium salt at pH 8	~68.9	8.0	~12.7 [c]	~6.0 [d]	[16]
TFC, flat sheet (HTI)	AL-FS	2.2 M $MgCl_2$	~163	5.43	~6.5 [b]	~9 [d]	[21]

[a] Osmotic pressure of the draw at room temperature (23°C) was estimated by using van't Hoff equation, where the van't Hoff factor of NaCl, $MgCl_2$, $CaCl_2$, $NaHSO_4$, Na_2SO_4 and EDTA sodium salt were taken as 2, 3, 3, 2, 3 and 4. Note that the estimated values may only be valid for dilute solutions.
[b] Final MLSS after 5 h of FO sludge thickening experiments were calculated from reported initial MLSS and volume reduction of sludge, where the latter was estimated from the figures.
[c] Final MLSS after 5 h of FO experiments were estimated from the figures.
[d] FO water flux after 5 h of FO experiments were estimated from the figures.

In order to further investigate the effect of the pore size of shell side skin layer on the fouling resistance of the FO membrane in sludge thickening process, parallel experiments were also carried out by using hollow fiber TFC membranes spun without purposefully densified outer skin layer, denoted as PES-PSHF-TFC (with a PWP of 262 LMH/bar and MWCO of 32 kDa, characterized by outside-in filtration experiments). The performance of the PES-PSHF-TFC membrane is shown together with the dual-skinned membrane in Figure 7.

Under the same testing conditions, PES-PSHF-TFC membrane exhibit much higher initial water flux but experienced more serious water flux decline over the first hour of FO experiments when using sludge as feed. Both membranes exhibit similar patterns of water flux decline over the next few hours as shown in Figure 7 (a-b). The observed water flux decline may be attributed to increase in resistance of the membrane due to accumulation of foulants, which could be estimated by simplified equation derived from Darcy's Law:

$$\Delta R = \left(R_f - R_0\right) = \frac{\Delta P}{\mu} \cdot \left(\frac{1}{J_{w,t}} - \frac{1}{J_{w,0}}\right) = \frac{\Delta \pi}{\mu} \cdot \left(\frac{1}{J_{w,t}} - \frac{1}{J_{w,0}}\right) \quad (3)$$

where R_f and R_0 are the resistance of pristine membrane and fouled membrane, ΔP is the driving force across the membrane, μ is the viscosity of the water, $J_{w,o}$ and $J_{w,t}$ are the water flux of pristine membrane and the water flux of fouled membrane. For FO process, osmotic pressure difference ($\Delta \pi$) across the selective layer of TFC membrane is the sole driving force, which is estimated by van't Hoff's equation. As shown in Figure 7(c), the increase in resistance of PES-PSHF-TFC membrane was apparently higher than that of double-skinned membrane, which indicates that foulant accumulation in double-skinned membrane is indeed slower.

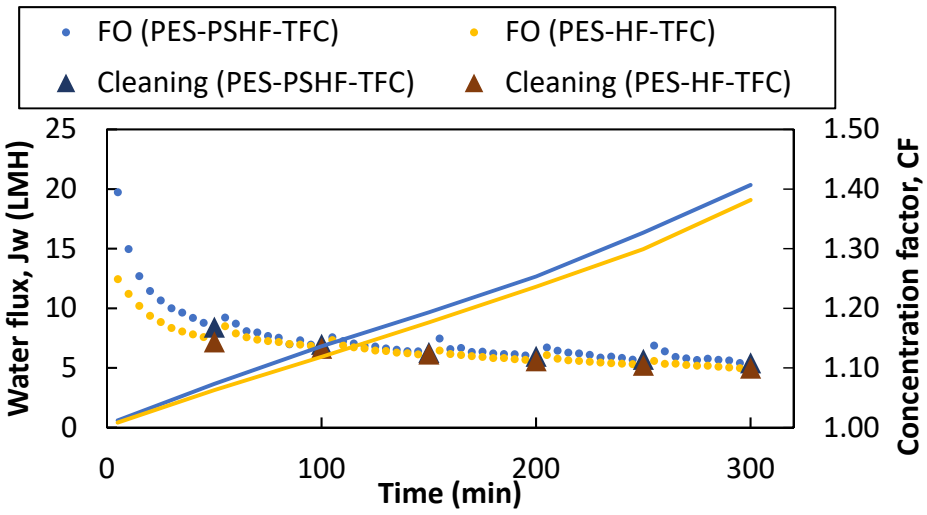

529

530 **(a)**

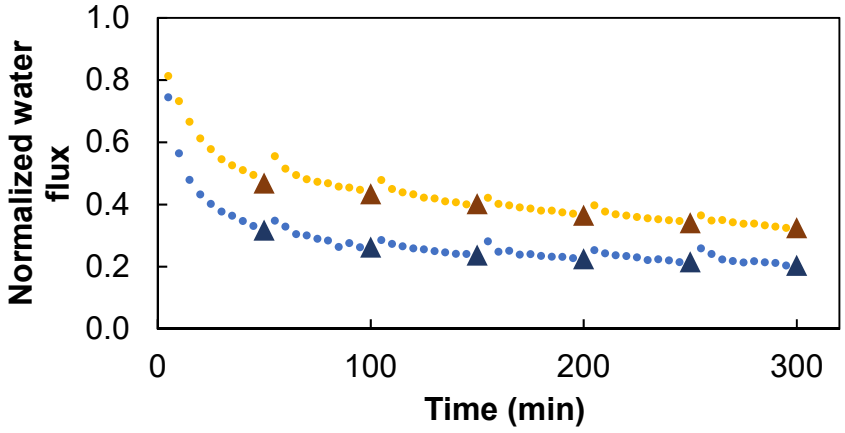

531

532 **(b)**

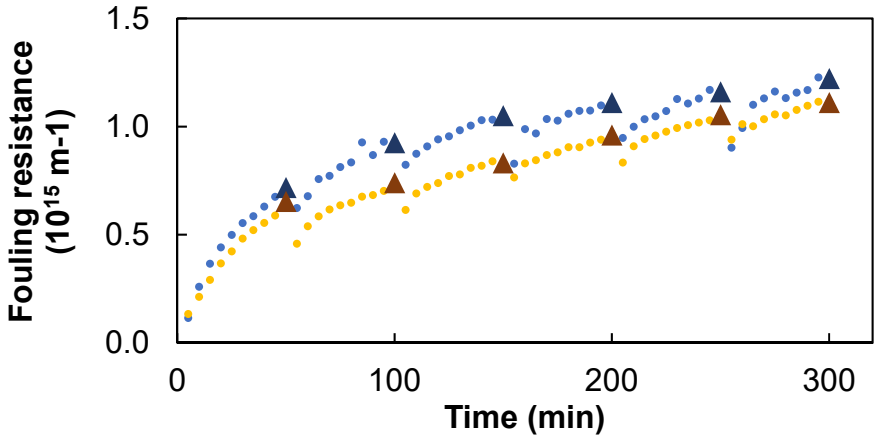

533

534 (c)

535 **Figure 7.** Water flux profiles (a), normalized water flux profiles (b), and apparent
536 resistance increment (c) of the PES-HF TFC membranes in sludge thickening
537 experiments (0.5 M NaCl as draw solution, crossflow velocity in membrane lumen side

538 at 0.8 m/s; 0.5 L of sludge at 15.5 g/L as feed, crossflow velocity in membrane shell
539 side at 0.23 m/s).

540

541 *3.3.2. Characteristics of irreversible foulants*

542 At the end of FO experiments (300-min), the physical-cleaned membranes were
543 removed from the module and the organic foulants accumulated inside of the FO
544 membrane was extracted by NaOH (pH 12, for 2h). The LC-OCD results (Figure 8)
545 revealed that the dense UF layer of the PES-HF-TFC membrane could effectively
546 reduce the accumulation of the higher molecular weight substances such as
547 biopolymers (>10 kDa), humic substances (~1 kDa), and building blocks (300-500 Da),
548 which were 370%, 130% and 130% lower than those in the feed sludge. However, low
549 molecular weight neutrals (<350 Da) tended to be accumulated inside of the FO
550 membrane, which was 70% higher than that in the feed sludge. This finding highlights
551 the importance in further minimizing the surface pore size of the secondary rejection
552 layer of FO membranes in order to improve rejection efficiency of low molecular weight
553 substances from the sludge samples.

554

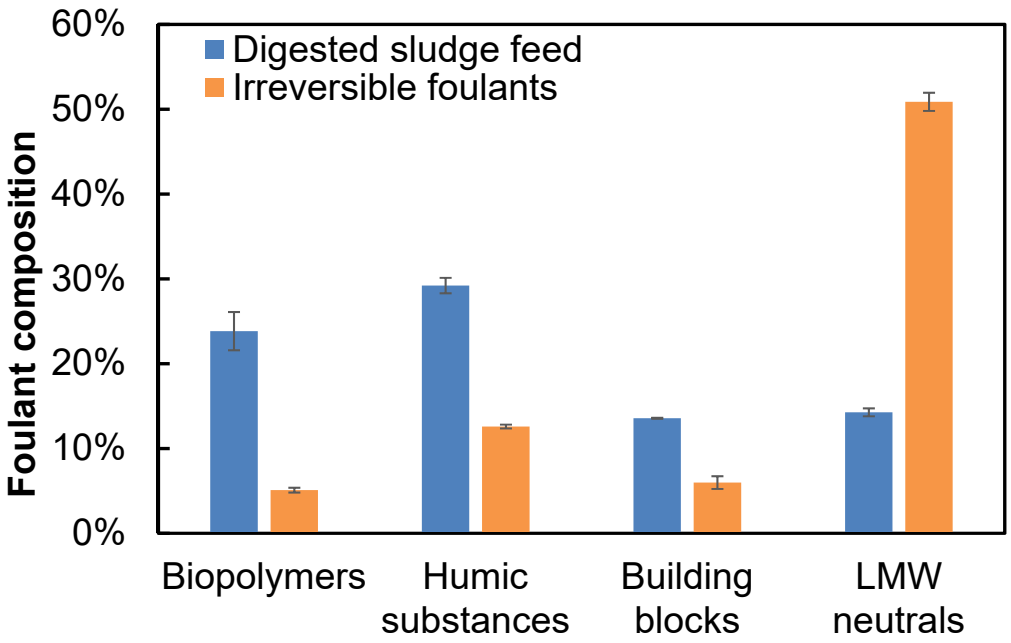

555

556 **Figure 8.** Composition ratios of organic substances in the feed sludge and irreversible
557 foulants accumulated in the PES-HF-TFC membrane.

558

559 Organic foulant analysis was also carried out by using PES-PSHF-TFC membrane
560 that has been tested in parallel experiments as PES-HF-TFC membrane as depicted
561 in Figure 9. It was found that higher amount of organic foulants could be extracted
562 from the former after sludge thickening experiments, as compared to the latter. In
563 terms of foulant composition, it appears that the accumulation of humic acid in PES-
564 PSHF-TFC membrane was much more significant. This observation confirmed that
565 the use of TFC membrane with smaller pore size on the shell side could effectively
566 reduced the deposition of high to medium molecular weight organic foulants in the
567 membrane.

568

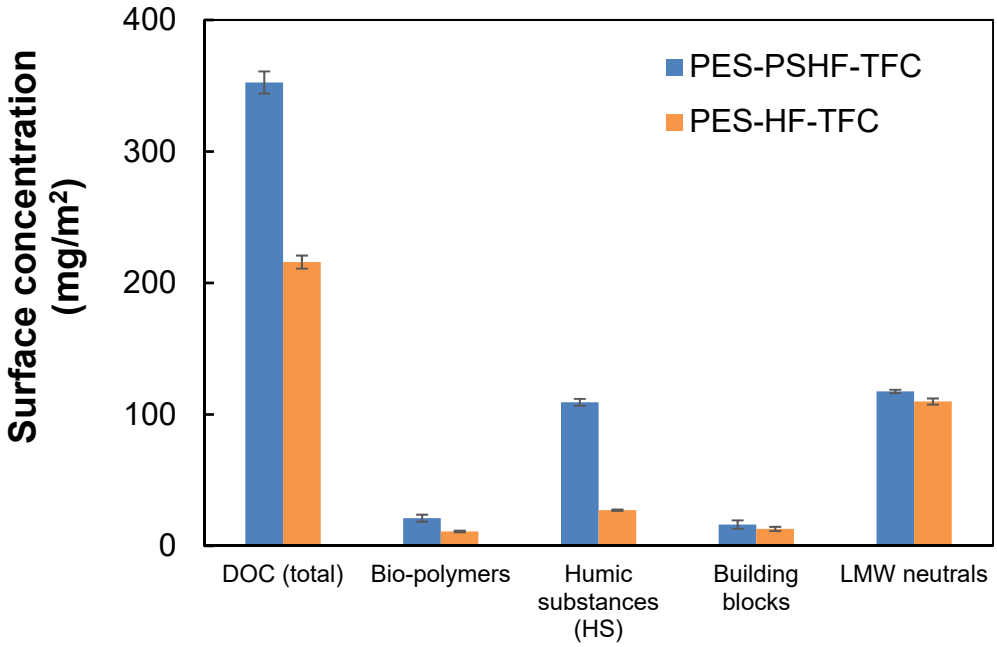

Figure 9. Compositions of organic foulants from both FO membranes.

4. Conclusions

This study developed a novel double-skinned (tight UF outer skin and RO inner skin) hollow fiber TFC FO membrane preparation process, i.e., fabricating a dual-layer PES substrate in one step, followed by interfacial polymerization of the inner-selective layer. This membrane exhibited better performance in concentrating humic acid and activated sludge in the AL-DS orientation as compared to most of the commercial membranes and some self-prepared membranes reported so far. The tight UF-like outer layer has proven to reject greater-sized molecules, for example, reducing the accumulations of biopolymers, humic acids, and building blocks inside of the FO membranes in sludge thickening processes, and thus helps to suppress irreversible organic fouling of the membranes.

Acknowledgements

584 The Economic Development Board (EDB) of Singapore is acknowledged for funding
585 the Singapore Membrane Technology Centre (SMTC), Nanyang Technological
586 University.

587

588 **References:**

589 [1] Y.-N. Wang, K. Goh, X. Li, L. Setiawan, R. Wang, Membranes and processes for
590 forward osmosis-based desalination: Recent advances and future prospects,
591 Desalination, 434 (2018) 81-99.
592 [2] A.G. Fane, R. Wang, M.X. Hu, Synthetic Membranes for Water Purification:
593 Status and Future, Angewandte Chemie International Edition, 54 (2015) 3368-3386.
594 [3] Y. Kim, M. Elimelech, H.K. Shon, S. Hong, Combined organic and colloidal
595 fouling in forward osmosis: Fouling reversibility and the role of applied pressure,
596 Journal of Membrane Science, 460 (2014) 206-212.
597 [4] W. Cheng, X. Lu, Y. Yang, J. Jiang, J. Ma, Influence of composition and
598 concentration of saline water on cation exchange behavior in forward osmosis
599 desalination, Water Research, 137 (2018) 9-17.
600 [5] M. Tian, Y.-N. Wang, R. Wang, Synthesis and characterization of novel high-
601 performance thin film nanocomposite (TFN) FO membranes with nanofibrous
602 substrate reinforced by functionalized carbon nanotubes, Desalination, 370 (2015)
603 79-86.
604 [6] E. Arkhangelsky, S. Sulaiman Lay, F. Wicaksana, A.A. Al-Rabiah, S.M. Al-
605 Zahrani, R. Wang, Impact of intrinsic properties of foulants on membrane
606 performance in osmotic desalination applications, Separation and Purification
607 Technology, 123 (2014) 87-95.
608 [7] R. Valladares Linares, Z. Li, S. Sarp, S.S. Bucs, G. Amy, J.S. Vrouwenvelder,
609 Forward osmosis niches in seawater desalination and wastewater reuse, Water
610 Research, 66 (2014) 122-139.
611 [8] B. Corzo, T. de la Torre, C. Sans, E. Ferrero, J.J. Malfeito, Evaluation of draw
612 solutions and commercially available forward osmosis membrane modules for

613 wastewater reclamation at pilot scale, Chemical Engineering Journal, 326 (2017) 1-
614 8.
615 [9] G. Chen, R. Liu, H.K. Shon, Y. Wang, J. Song, X.-M. Li, T. He, Open porous
616 hydrophilic supported thin-film composite forward osmosis membrane via co-casting
617 for treatment of high-salinity wastewater, Desalination, 405 (2017) 76-84.
618 [10] S.M. Iskander, J.T. Novak, Z. He, Enhancing forward osmosis water recovery
619 from landfill leachate by desalinating brine and recovering ammonia in a microbial
620 desalination cell, Bioresource Technology, 255 (2018) 76-82.
621 [11] L.D. Banchik, A.M. Weiner, B. Al-Anzi, J.H. Lienhard V, System scale analytical
622 modeling of forward and assisted forward osmosis mass exchangers with a case
623 study on fertigation, Journal of Membrane Science, 510 (2016) 533-545.
624 [12] D.I. Kim, J. Choi, S. Hong, Evaluation on suitability of osmotic dewatering
625 through forward osmosis (FO) for xylose concentration, Separation and Purification
626 Technology, 191 (2018) 225-232.
627 [13] Y.-N. Wang, R. Wang, W. Li, C.Y. Tang, Whey recovery using forward osmosis
628 – Evaluating the factors limiting the flux performance, Journal of Membrane Science,
629 533 (2017) 179-189.
630 [14] E.M. Garcia-Castello, J.R. McCutcheon, Dewatering press liquor derived from
631 orange production by forward osmosis, Journal of Membrane Science, 372 (2011)
632 97-101.
633 [15] N.C. Nguyen, H.T. Nguyen, S.-S. Chen, N.T. Nguyen, C.-W. Li, Application of
634 forward osmosis (FO) under ultrasonication on sludge thickening of waste activated
635 sludge, Water Science and Technology, 72 (2015) 1301-1307.
636 [16] N.T. Hau, S.-S. Chen, N.C. Nguyen, K.Z. Huang, H.H. Ngo, W. Guo, Exploration
637 of EDTA sodium salt as novel draw solution in forward osmosis process for

638 dewatering of high nutrient sludge, Journal of Membrane Science, 455 (2014) 305-
639 311.
640 [17] N.C. Nguyen, S.-S. Chen, H.-Y. Yang, N.T. Hau, Application of forward osmosis
641 on dewatering of high nutrient sludge, Bioresource Technology, 132 (2013) 224-229.
642 [18] H. Zhu, L. Zhang, X. Wen, X. Huang, Feasibility of applying forward osmosis to
643 the simultaneous thickening, digestion, and direct dewatering of waste activated
644 sludge, Bioresource Technology, 113 (2012) 207-213.
645 [19] M. Collard, B. Teychené, L. Lemée, Comparison of three different wastewater
646 sludge and their respective drying processes: Solar, thermal and reed beds – Impact
647 on organic matter characteristics, Journal of Environmental Management, 203 (2017)
648 760-767.
649 [20] H. Ge, P.D. Jensen, D.J. Batstone, Pre-treatment mechanisms during
650 thermophilic–mesophilic temperature phased anaerobic digestion of primary sludge,
651 Water Research, 44 (2010) 123-130.
652 [21] C. Cagnetta, A. D'Haese, M. Coma, R. Props, B. Buysschaert, A.R.D. Verliefde,
653 K. Rabaey, Increased carboxylate production in high-rate activated A-sludge by
654 forward osmosis thickening, Chemical Engineering Journal, 312 (2017) 68-78.
655 [22] T.M. Missimer, R.G. Maliva, Environmental issues in seawater reverse osmosis
656 desalination: Intakes and outfalls, Desalination, 434 (2018) 198-215.
657 [23] L. Meng, M. Huang, L. Bi, T. Cai, Y. Huang, Performance of simultaneous
658 wastewater reuse and seawater desalination by PAO-LPRO process, Separation
659 and Purification Technology, 201 (2018) 276-282.
660 [24] N.T. Hancock, P. Xu, M.J. Roby, J.D. Gomez, T.Y. Cath, Towards direct potable
661 reuse with forward osmosis: Technical assessment of long-term process
662 performance at the pilot scale, Journal of Membrane Science, 445 (2013) 34-46.

663 [25] R. Wang, L. Shi, C.Y. Tang, S. Chou, C. Qiu, A.G. Fane, Characterization of
664 novel forward osmosis hollow fiber membranes, Journal of Membrane Science, 355
665 (2010) 158-167.
666 [26] J. Su, T.-S. Chung, B.J. Helmer, J.S. de Wit, Enhanced double-skinned FO
667 membranes with inner dense layer for wastewater treatment and macromolecule
668 recycle using Sucrose as draw solute, Journal of Membrane Science, 396 (2012) 92-
669 100.
670 [27] W. Fang, R. Wang, S. Chou, L. Setiawan, A.G. Fane, Composite forward
671 osmosis hollow fiber membranes: Integration of RO- and NF-like selective layers to
672 enhance membrane properties of anti-scaling and anti-internal concentration
673 polarization, Journal of Membrane Science, 394 (2012) 140-150.
674 [28] W. Fang, C. Liu, L. Shi, R. Wang, Composite forward osmosis hollow fiber
675 membranes: Integration of RO- and NF-like selective layers for enhanced organic
676 fouling resistance, Journal of Membrane Science, 492 (2015) 147-155.
677 [29] G. Han, Z.L. Cheng, T.-S. Chung, Thin-film composite (TFC) hollow fiber
678 membrane with double-polyamide active layers for internal concentration polarization
679 and fouling mitigation in osmotic processes, Journal of Membrane Science, 523
680 (2017) 497-504.
681 [30] C.Y. Tang, Q. She, W.C.L. Lay, R. Wang, R. Field, A.G. Fane, Modeling double-
682 skinned FO membranes, Desalination, 283 (2011) 178-186.
683 [31] S. Qi, C.Q. Qiu, Y. Zhao, C.Y. Tang, Double-skinned forward osmosis
684 membranes based on layer-by-layer assembly—FO performance and fouling
685 behavior, Journal of Membrane Science, 405 (2012) 20-29.

686 [32] L. Setiawan, R. Wang, L. Shi, K. Li, A.G. Fane, Novel dual-layer hollow fiber
687 membranes applied for forward osmosis process, Journal of Membrane Science,
688 421 (2012) 238-246.
689 [33] X. Li, C.H. Loh, R. Wang, W. Widjajanti, J. Torres, Fabrication of a robust high-
690 performance FO membrane by optimizing substrate structure and incorporating
691 aquaporin into selective layer, Journal of Membrane Science, 525 (2017) 257-268.
692 [34] Z.L. Cheng, X. Li, Y.D. Liu, T.-S. Chung, Robust outer-selective thin-film
693 composite polyethersulfone hollow fiber membranes with low reverse salt flux for
694 renewable salinity-gradient energy generation, Journal of Membrane Science, 506
695 (2016) 119-129.
696 [35] S. Singh, K.C. Khulbe, T. Matsuura, P. Ramamurthy, Membrane
697 characterization by solute transport and atomic force microscopy, Journal of
698 Membrane Science, 142 (1998) 111-127.
699 [36] Y. Chen, L. Setiawan, S. Chou, X. Hu, R. Wang, Identification of safe and stable
700 operation conditions for pressure retarded osmosis with high performance hollow
701 fiber membrane, Journal of Membrane Science, 503 (2016) 90-100.
702 [37] S. Chou, R. Wang, A.G. Fane, Robust and High performance hollow fiber
703 membranes for energy harvesting from salinity gradients by pressure retarded
704 osmosis, Journal of Membrane Science, 448 (2013) 44-54.
705 [38] X. Li, S. Chou, R. Wang, L. Shi, W. Fang, G. Chaitra, C.Y. Tang, J. Torres, X.
706 Hu, A.G. Fane, Nature gives the best solution for desalination: Aquaporin-based
707 hollow fiber composite membrane with superior performance, Journal of Membrane
708 Science, 494 (2015) 68-77.

709 [39] L.S. Clesceri, A.E. Greenberg, A.D. Eaton, Standard Methods for the
710 Examination of Water and Wastewater, 20th Edition, APHA American Public Health
711 Association1998.
712 [40] S.A. Huber, A. Balz, M. Abert, W. Pronk, Characterisation of aquatic humic and
713 non-humic matter with size-exclusion chromatography – organic carbon detection –
714 organic nitrogen detection (LC-OCD-OND), Water Research, 45 (2011) 879-885.
715 [41] D. Li, T.-S. Chung, R. Wang, Morphological aspects and structure control of
716 dual-layer asymmetric hollow fiber membranes formed by a simultaneous co-
717 extrusion approach, Journal of Membrane Science, 243 (2004) 155-175.
718 [42] S.P. Sun, K.Y. Wang, N. Peng, T.A. Hatton, T.-S. Chung, Novel polyamide-
719 imide/cellulose acetate dual-layer hollow fiber membranes for nanofiltration, Journal
720 of Membrane Science, 363 (2010) 232-242.
721 [43] C. Barth, M.C. Gonçalves, A.T.N. Pires, J. Roeder, B.A. Wolf, Asymmetric
722 polysulfone and polyethersulfone membranes: effects of thermodynamic conditions
723 during formation on their performance, Journal of Membrane Science, 169 (2000)
724 287-299.
725 [44] S.S. Prakash, L.F. Francis, L.E. Scriven, Microstructure evolution in dry–wet
726 cast polysulfone membranes by cryo-SEM: A hypothesis on macrovoid formation,
727 Journal of Membrane Science, 313 (2008) 135-157.
728 [45] A. Cassano, C. Conidi, R. Ruby-Figueroa, R. Castro-Muñoz, Nanofiltration and
729 Tight Ultrafiltration Membranes for the Recovery of Polyphenols from Agro-Food By-
730 Products, International Journal of Molecular Sciences, 19 (2018) 351.
731 [46] D. Jermann, W. Pronk, S. Meylan, M. Boller, Interplay of different NOM fouling
732 mechanisms during ultrafiltration for drinking water production, Water Research, 41
733 (2007) 1713-1722.

734 [47] S. Shao, H. Liang, F. Qu, K. Li, H. Chang, H. Yu, G. Li, Combined influence by
735 humic acid (HA) and powdered activated carbon (PAC) particles on ultrafiltration
736 membrane fouling, Journal of Membrane Science, 500 (2016) 99-105.
737 [48] G. Han, T.-S. Chung, Robust and high performance pressure retarded osmosis
738 hollow fiber membranes for osmotic power generation, AIChE Journal, 60 (2014)
739 1107-1119.
740 [49] X. Song, L. Wang, C.Y. Tang, Z. Wang, C. Gao, Fabrication of carbon
741 nanotubes incorporated double-skinned thin film nanocomposite membranes for
742 enhanced separation performance and antifouling capability in forward osmosis
743 process, Desalination, 369 (2015) 1-9.
744 [50] C.Y. Tang, Q. She, W.C.L. Lay, R. Wang, A.G. Fane, Coupled effects of internal
745 concentration polarization and fouling on flux behavior of forward osmosis
746 membranes during humic acid filtration, Journal of Membrane Science, 354 (2010)
747 123-133.
748 [51] K. Katsoufidou, S.G. Yiantsios, A.J. Karabelas, A study of ultrafiltration
749 membrane fouling by humic acids and flux recovery by backwashing: Experiments
750 and modeling, Journal of Membrane Science, 266 (2005) 40-50.
751 [52] C. Jönsson, A.-S. Jönsson, Influence of the membrane material on the
752 adsorptive fouling of ultrafiltration membranes, Journal of Membrane Science, 108
753 (1995) 79-87.
754 [53] M. Kawahigashi, N. Fujitake, H. Yajima, H. Sumida, Particle sizes of standard
755 humic substances calculated as radii of gyration, maximum diameter and
756 hydrodynamic radii, Humic Subst Res, 8 (2011) 13-18.
757 [54] J. Heo, K.H. Chu, N. Her, J. Im, Y.-G. Park, J. Cho, S. Sarp, A. Jang, M. Jang,
758 Y. Yoon, Organic fouling and reverse solute selectivity in forward osmosis: Role of

759 working temperature and inorganic draw solutions, Desalination, 389 (2016) 162-
760 170.
761 [55] T. Majeed, S. Phuntsho, S. Jeong, Y. Zhao, B. Gao, H.K. Shon, Understanding
762 the risk of scaling and fouling in hollow fiber forward osmosis membrane application,
763 Process Safety and Environmental Protection, 104 (2016) 452-464.
764 [56] M. Xie, L.D. Nghiem, W.E. Price, M. Elimelech, Impact of organic and colloidal
765 fouling on trace organic contaminant rejection by forward osmosis: Role of initial
766 permeate flux, Desalination, 336 (2014) 146-152.
767 [57] M. Xie, L.D. Nghiem, W.E. Price, M. Elimelech, Toward Resource Recovery
768 from Wastewater: Extraction of Phosphorus from Digested Sludge Using a Hybrid
769 Forward Osmosis–Membrane Distillation Process, Environmental Science &
770 Technology Letters, 1 (2014) 191-195.

771

772

773